FULL PAPER

Investigation of Optical and Structural Stability of Localized Surface Plasmon Mediated Light-Emitting Diodes by Ag and Ag/SiO_2 Nanoparticles

*Lee-Woon Jang, Dae-Woo Jeon, Myoung Kim, Ju-Won Jeon, Alexander Y. Polyakov, Jin-Woo Ju, Seung-Jae Lee, Jong-Hyeob Baek, Jin-Kyu Yang, and In-Hwan Lee**

Localized surface plasmon (LSP) effects due to Ag and Ag/SiO_2 nanoparticles (NPs) deposited on GaN/InGaN multiquantum well (MQW) light-emitting diode (LED) structures are studied. The colloidal NPs are synthesized by a sol-gel method and drop-cased on the LED structures. The surface density of NPs its controlled by the concentration of the NP solution. Theoretical modeling is performed for the emission spectrum and the electric field distribution of LSP resonance for Ag/SiO_2 NPs. Enhanced photoluminescence (PL) efficiency is observed in the LED structures and the amount of PL enhancement increases with increasing the surface density of Ag and Ag/SiO_2 NPs. These effects are attributed to resonance coupling between the MQW and LSP in the NPs. It is also shown that the PL enhancement attainable with Ag NPs and Ag/SiO_2 NPs is comparable, but the latter displays a much higher stability with respect to long-term storage and annealing due to a barrier for NP agglomeration, Ag oxidation, and impurity diffusion provided by the SiO_2 shell.

1. Introduction

Surface plasmons (SPs) are coherent electron oscillations that exist at a metal/dielectric interface. Specifically, the SPs in noble metal nanoparticles (NPs) embedded in a dielectric matrix are called localized surface plasmons (LSPs).[1,2] The unique optical properties of LSPs have been studied for applications in sensing, imaging, surface enhanced spectroscopy, solar cells, and light-emitting diodes (LEDs).[3–6] The LSPs extend its distribution of near-field electromagnetic field into the dielectric side for several tens of nanometer.[7] At shorter distances of below 10 nm the Forster resonant energy transfer mechanism based on dipole–dipole interaction is operative,[8] while for very short distances from light-emitting layers the light emission is generally quenched due to quantum mechanical tunneling effects.[9] The applications of LSP properties also depend on the degree of peak energy matching between the resonance energy of LSPs and the emission energy of a light emitter (a dipole or an electron–hole pair).[10,11] The resonant wavelength of LSPs is determined by the shape, size, type, and structure of metal.[2,6,10] Usually, the Ag and Au NPs are applied in the blue and green wavelength regions, respectively.[6]

If a light emitter is placed in close proximity to NPs and its energy is coincident with LSP frequency, an effective energy transfer takes place from the emitter to LSPs.[6] Once transferred, the energy excites the LSPs, which can effectively radiate into photons.[12] Likewise, LSP-mediated LED structures can be realized by placing the metal NPs close to the energy-matched active layer within the penetration depth of LSP field. The spatial overlap of this near field with the quantum well (QW) layer results in a LSP coupling effect by which the energy of light emitter is resonantly transferred into LSPs for emission to create an alternative efficient emission channel.[11,13,14] This additional highly effective recombination channel competes against the non-radiative recombination processes in the QW region and increases the light emission efficiency.[10–15] The internal quantum efficiency (IQE) of the LED is given by $\eta_{int} = (k_{rad} + k_{LSP})/(k_{rad} + k_{non} + k_{LSP})$, where k_{rad} and k_{non} are the radiative and non-radiative recombination rates of electron-hole pairs and k_{LSP} is the coupling rate between active layer and LSPs.[6] IQE can be therefore greatly improved due to the operation of the k_{LSP} term. In well-prepared NPs, spontaneous emission into LSPs is several tens of times faster than normal spontaneous emission from InGaN QW.[12,15,16]

Okamoto et al.[6] first explored SPs in terms of SP polaritons in the rough (or grated) silver film coated on InGaN QW and

L.-W. Jang, D.-W. Jeon, M. Kim, J.-W. Jeon, A. Y. Polyakov, Prof. I.-H. Lee
School of Advanced Materials Engineering and Research Center of Advanced Materials Development and Semiconductor Physics Research Center
Chonbuk National University
Jeonju 561-756, Korea
E-mail: ihlee@jbnu.ac.kr
Dr. J.-W. Ju, Dr. S.-J. Lee, Dr. J.-H. Baek
LED Device Team, Korea Photonics Technology Institute
Gwangju 500-779, Korea
Prof. J.-K. Yang
Department of Optical Engineering
Kongju National University
Kongju, Chungnam 314-701, Korea

DOI: 10.1002/adfm.201103161

reported a 6.8 times increase of the IQE, fueling research for realizing SP-mediated LEDs. In comparison with the SPs in the continuous metal films that have fundamental shortcomings,[17] the LSPs in metal NPs are becoming increasingly studied due to their unique advantages and the recent improvements in NP synthesis and low cost fabrication processes.[15–19] Photoluminescence (PL) intensity enhancement due to LSP-QW coupling was demonstrated for GaN/InGaN multi-quantum well (MQW) LED structures with thin spacer layer and NPs deposited on top.[6,16] LSP-enhanced electroluminescence (EL) intensity was reported for NPs embedded in p-type GaN top layer or in n-type GaN underlying the MQW region of LED.[7,11–14] Recently, we reported the observation of LSP phenomena for Ag/SiO_2 NPs and the enhancement of PL emission due to deposition of such NPs on GaN/InGaN LED structures.[15] With theoretical calculations, we suggested that the PL enhancement by LSPs is also related to the interaction between individual metal NPs because the electric fields of individual neighboring NPs can strongly affect the LSP efficiency.[3,18,19] This indicates that the concentration of Ag/SiO_2 NPs can have an impact on the luminescence efficiency of LSPs.

Here, we describe the results of experimental and theoretical studies of the optical properties and electric field distribution in Ag and Ag/SiO_2 NPs as a function of their dimensions and report on the coupling efficiency of their LSP resonance with GaN/InGaN MQW. We also present initial research on relative thermal stability of Ag/SiO_2 NPs compared to Ag NPs, demonstrating inherent advantages of the former in obtaining robust LSP-mediated emission enhancement from the LED structure.

2. Result and Discussion

It is known that the emission intensity of radiation sources located within the near field region of LSPs can be strongly enhanced if the emission wavelength is reasonably well matched to the wavelength of the LSP resonance. To obtain the spatial distribution of the LSP electric field strength in the vicinity of NPs we performed the full three-dimensional (3D) finite-difference time-domain (FDTD) simulation. For the chosen sample and NP characteristics the optical properties of NPs near emission energy (470 nm) were determined using the Drude equation and the data in ref. [20,21] **Figure 1**a shows the electric field distribution for a set of parameters: 7 Ag/SiO_2 NPs with 30 nm Ag in diameter and 20 nm thick SiO_2 (refractive index, $n = 1.55$), 10 nm thick GaN spacer ($n = 2.3$) and 470 nm emission peak for the InGaN MQW. Figure 1b displays the LSP resonance emission spectrum for NPs of these dimensions and structure. It can be seen from Figure 1a that the electric field of seven Ag/SiO_2 NPs is strongly confined near the surface of NPs, but the field penetrates deeper beyond the InGaN MQW region.[6,22] The emission spectrum due to the LSP resonance clearly exhibits a strong peak in the blue wavelength region suitable for matching to the MQW emission peak (Figure 1b). Numerical simulation also shows that the strength of resonance is increased when increasing the number of NPs (see e.g., ref. [15]). Thus, theoretical modeling suggests that our sol-gel synthesized Ag/SiO_2 NPs are of great potential interest for

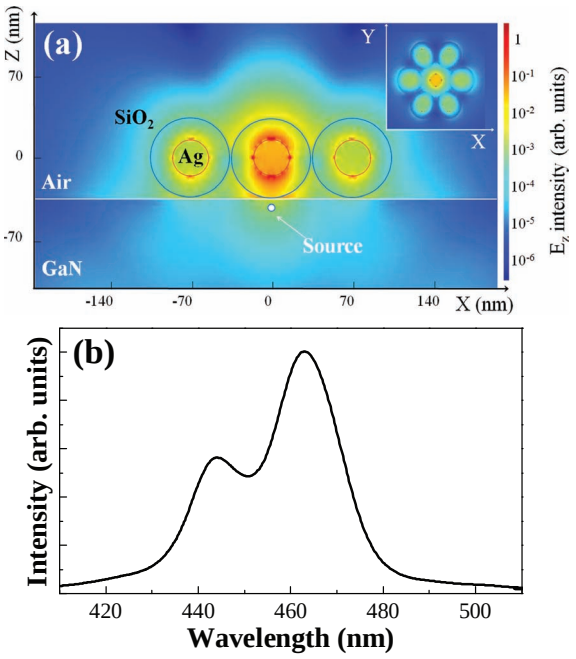

Figure 1. Electric field distribution of LSP mode (a) and emission spectrum (b) from the 7 Ag/SiO_2 NPs after source radiation. The inset shows a plan view of the field distribution. The diameter of Ag core is 30 nm and the thickness of SiO_2 shell is 20 nm.

LSP enhancement of the blue InGaN/GaN MQW LED. Experimental results presented below support this conclusion.

Typical transmission electron microscopy (TEM) images of Ag and Ag/SiO_2 NPs synthesized by sol-gel method are shown in **Figure 2**. Figure 2a shows the image of the Ag NPs (gray spheres with diameter of around 30 nm) while Figure 2b displays the image of the Ag/SiO_2 NPs with Ag cores, 30 nm in diameter, seen as darker shade of gray and surrounded by 20–25 nm thick SiO_2 shells visible as lighter regions. The density of NPs can be increased approximately linearly by decreasing the solvent volume with a fixed solute amount after the centrifugation process. About 10 μL of colloidal solution was directly coated on the surface of the LED structure by drop-casting and was subjected to a very short (several seconds) drying at 100 °C to remove the solvent. Three different solutions were prepared for each of Ag NPs (A,B,C) and Ag/SiO_2 NPs (D,E,F) with the concentrations varied by an order of magnitude in the row. Figure 2c displays characteristic coloring of respective reagents solutions. The samples coated with solution A and D showed discrete and sparse single layers of NPs. The solution B and E coated samples displayed almost continuous single layer of NPs, while C and F coated samples exhibited an irregular pile of NPs. Here the estimated Ag NP densities on LED surface are 4.7×10^8 cm^{-2} (A), 6.0×10^9 cm^{-2} (B) and 4.9×10^{10} cm^{-2} (C). In the Ag/SiO_2 NP case they are 1.7×10^8 cm^{-2} (D), 2.3×10^9 cm^{-2} (E), and 1.7×10^{10} cm^{-2} (F).

The effects of NP deposition on the emission intensity of GaN/InGaN MQW LED structures were examined by PL measurements with the back-side excitation geometry and the PL results are presented in **Figure 3**a. Compared to the reference

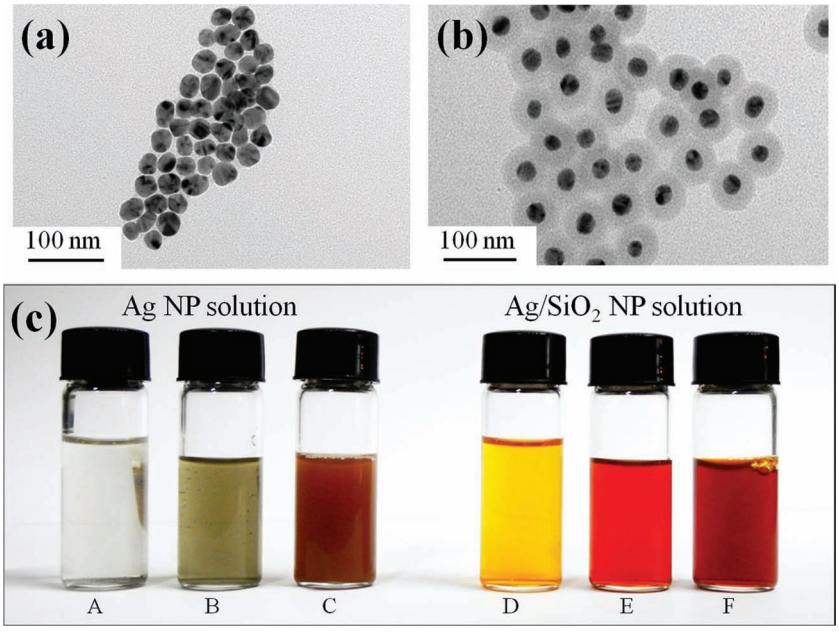

Figure 2. TEM images (a,b) and photograph (c) of the Ag and Ag/SiO_2 NPs synthesized by sol-gel method. The diameter of Ag core is around 30–40 nm and the thickness of SiO_2 shell is around 20–25 nm. The resulting Ag NP densities on LED surface are 4.7×10^8 cm^{-2} (A), 6.0×10^9 cm^{-2} (B), and 4.9×10^{10} cm^{-2} (C). In the Ag/SiO_2 NP case they are 1.7×10^8 cm^{-2} (D), 2.3×10^9 cm^{-2} (E), and 1.7×10^{10} cm^{-2} (F).

sample (with the PL enhancement ratio set to 100%) the PL intensities for the samples coated with Ag and Ag/SiO_2 NPs were increased and the enhancement ratio was also increased with increasing the density of NPs (Figure 3a). The improved PL efficiency is attributed to the product of light extraction efficiency[23] and IQE.[6] In order to indentify the origin of PL enhancement in our LED structures, the PL yields were compared for the samples coated with SiO_2 NPs (without Ag core), Ag NPs, and Ag/SiO_2 NPs, as seen in Figure 3b. For planar LED structures, the extraction efficiency is low because the difference between the refractive index of GaN and air is large, and the critical angle of total internal reflection is calculated to be only around 23°. For all higher angles the light cannot leave the LED structure. SiO_2 NPs on the GaN surface promote the light scattering at the surface and also slightly increase the effective critical angle (the critical angle from GaN via SiO_2 to the air is 25.2°, which is slightly larger than 23.6° for the GaN/air interface[24]). Corresponding PL intensity increase is 1.3 times, which gives us an estimate of contribution due to better light extraction. In the case of the Ag and Ag/SiO_2 NP coated sample the magnitude of PL enhancement is higher and should be attributed to the enhanced IQE due to the LSP resonance coupling by the NPs. The IQE of conventional LED is limited by the defects such as threading dislocations that increase the non-radiative recombination rate and thus reduce the internal quantum efficiency. LSPs create an additional recombination channel with a very high photon density of states that competes with the non-radiative recombination channel and effectively increases the IQE.[25] The amount of PL enhancement due to this mechanism can be estimated by comparing the ratio of PL intensities at room temperature and at low temperature (10 K in our case). If one assumes, as is customary, that at low temperature the IQE is equal to 100% this ratio gives the IQE value at room temperature. For both the reference sample and the SiO_2 NP coated sample, the IQE value was the same, close to 21%, i.e., SiO_2 coating does not change appreciably the IQE. This indicates that the PL enhancement at room temperature observed for this sample is solely due to improved light extraction. For the Ag and Ag/SiO_2 NP coated samples the IQE was found to increase to approximately 30%, indicative of IQE enhancement (by ≈50%) by LSP–photon coupling. It means that the energy of excited carriers is transferred to the LSP of the NPs before being captured by non-radiative recombination center and thus increases IQE. PL intensity relaxation curves measured by time-resolved PL (TRPL) for photon energies corresponding to the PL spectra peak give additional proof of the validity of the proposed mechanisms. Figure 3c presents such decay curves for all studied types of samples. All relaxation curves show an initial fast decay region as usual for GaN/InGaN MQW.[10,26] Characteristic lifetimes for the reference and SiO_2 NPs coated samples in this region were 1.38 ns and 1.05 ns, respectively. A slightly shorter lifetime of the SiO_2 NP coated sample suggests the possibility of enhanced surface recombination process at the SiO_2/GaN interface.[26,27] The lifetimes of Ag/SiO_2 NPs and Ag NPs coated samples were estimated to be 480 ps and 227 ps, respectively. The combination of a shorter lifetime and enhanced PL intensity in the Ag and Ag/SiO_2 NP coated samples, compared to the reference and SiO_2 coated samples, indicates that shorter lifetimes in the former two cases are not a consequence of enhanced non-radiative relaxation process and that these effects are rather related to the increase in the spontaneous emission rate by the coupling between the carriers in MQW and the LSPs in NPs.

One more factor that has to be considered here is the stability of the observed PL enhancement due to NPs. Typically, in the LED under operation conditions, the temperature of the active region can reach up to 150 °C due to the Joule heating by the current injection.[28] Therefore, it is crucial to understand the nature of changes in the properties of the NP coatings during LED operation; this change can affect the physical and chemical characteristics of NPs and impact the stability of the PL enhancement. Two effects seem to be of particular importance for NPs being at an elevated temperature: size change and oxidation.[29] Until now only the effects of oxidation and LSP resonance frequency change for pure-metallic NPs have been studied,[30] but virtually nothing has been done for understanding the stability of LSP mediated enhancement of LED performance. Here, we present the results of structural, compositional and optical studies of Ag NPs with diameter of 30–40 nm and Ag/SiO_2 NPs with the similar Ag size and 20–25 nm thick SiO_2 shell. **Figure 4** shows SEM images of Ag (Figure 4a) and Ag/SiO_2 (Figure 4c) NPs after annealing

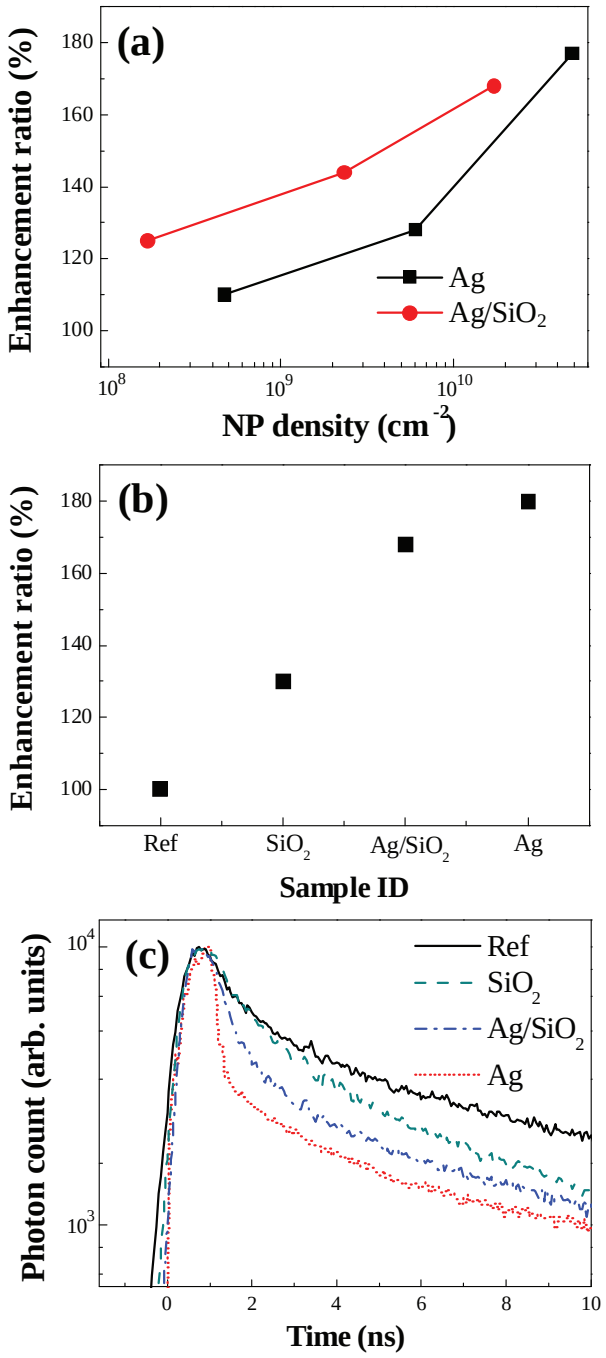

Figure 3. a) QW PL enhancement ratio for Ag and Ag/SiO_2 NPs with various NP density (Ag core: 30–40 nm in diameter, SiO_2 shell: 20–25 nm in thickness). b) PL enhancement measured for different types of NPs (SiO_2 NPs: 7.0×10^{10} cm^{-2}, Ag NPs: 4.9×10^{10} cm^{-2}, Ag/SiO_2 NPs: 1.7×10^{10} cm^{-2}). c) TRPL relaxation curves for the NP samples used in (b).

on hot-plate for 7 h at 100 °C in air and X-ray photoelectron spectroscopy (XPS) spectra before and after annealing (respectively, Figure 4b,d). After annealing, the Ag NPs, as shown in Figure 4a, agglomerated together to form large clusters of micrometer in diameter and the diameter tended to increase with annealing time (Figure 2a gives the dimensions of the NPs before the annealing; we use TEM imaging for reference here rather than SEM because of the very small size of as-deposited NPs). XPS spectra measured before and after annealing for the Ag NPs sample are presented in Figure 4b. The C 1s, O 1s, Ag 3d, and Ag 3p lines can be clearly seen. One can also observe a broad feature centered near 600 eV seemingly related to the Ag 3p line so that we somewhat tentatively attribute it to the Ag 3p line broadened and shifted in the mixed AgO-Ag_2O native oxide; this attribution is partly confirmed by the energy position of the O 1s line corresponding to the binding energy of O in Ag_2O.[31] The C 1s line of 284.5 eV binding energy was used as a reference to correct the binding energies for possible charge shifts.[29] The most obvious effect after the annealing is the very marked increase of the intensity of the O 1s peak and the intensity of the broad feature near 600 eV attributed above to the Ag 3p line in the native oxide. The amount of increase is much stronger than the increase in the intensity of the Ag 3d line that could be ascribed to increased Ag NP dimensions. These results show, in our view, that upon annealing not only the dimensions of Ag NPs increase, but also the thickness of the native oxide surrounding them does. These changes in NP dimensions and chemical composition measurably shift the LSP resonance to longer wavelength.[30,32,33] Consequently, the red-shift of LSP resonance has a decisive effect on the efficiency of the LED, as demonstrated below.

In the case of Ag/SiO_2 NPs, the shape was well preserved after annealing as shown in Figure 4c as compared to Figure 2b. At the same time, no remarkable changes in XPS spectra were observed for this sample after annealing suggesting that the chemical composition of the NPs was also not changed. Respective spectra are compared in Figure 4d. The O 1s peak in the figure is related to the binding energy of the SiO_2 shell and to Ag oxidation and it is difficult to discriminate between the AgO, Ag_2O, and SiO_2. However, much less variation of the peak energy width and intensity for annealed Ag/SiO_2 NPs compared to the result for Ag NPs indicates that the SiO_2 shell can protect the Ag core during annealing. That is, the Ag/SiO_2 NPs can keep the shape and prevent the Ag oxidation and the change of LSP resonance after annealing, while for Ag NPs the agglomeration and oxidation during annealing are serious issues and should affect the PL efficiency.

This is indeed confirmed by experiment using these Ag NPs (diameter: 30–40 nm) and Ag/SiO_2 NPs (SiO_2 thickness: 20–25 nm). **Figure 5** shows the PL efficiency variation as a function of annealing time in air. With increasing the exposure time, the PL intensity of Ag NP coated sample was sharply decreased and this is mainly caused by the LSP resonance change due to agglomeration and oxidation of Ag NPs. In contrast, the PL intensity of the Ag/SiO_2 NP coated sample changed very little after annealing due to small variations in the NP dimensions and oxidation. The reasons for the initial decrease of PL intensity with annealing time need yet to be understood.

The results above point to a much better thermal stability of Ag/SiO_2 NPs and the enhanced PL for LED structures coated with these NPs, compared to Ag NPs. This certainly is a serious advantage of the core/shell NPs. However, the amount of efficiency increase depends on the distance between the NP LSP resonant layer and the QW region of the LED structure. The

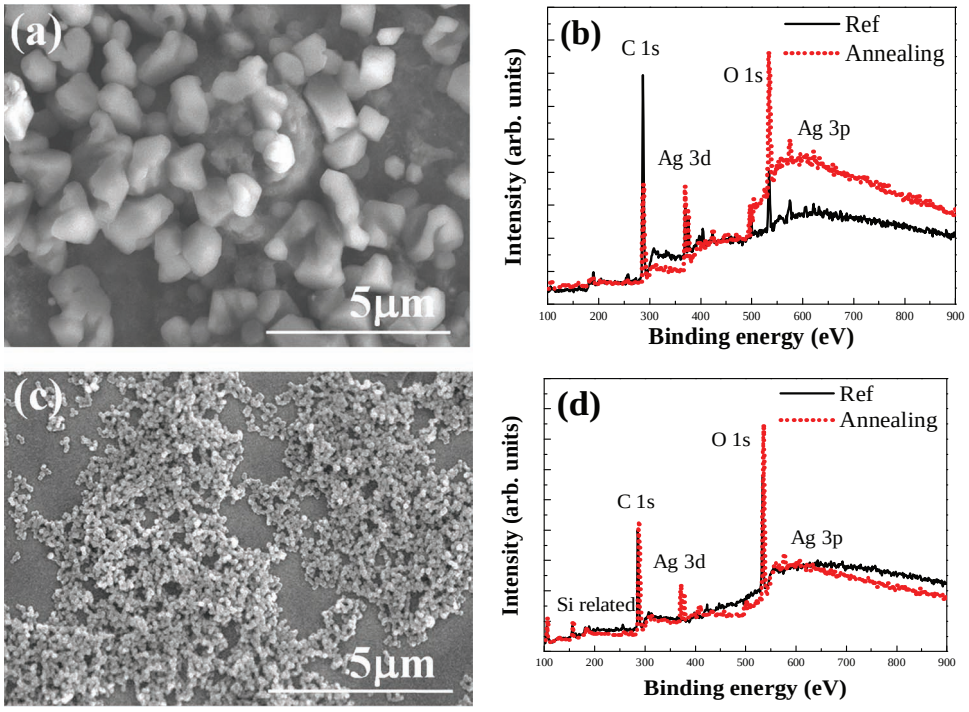

Figure 4. SEM images of Ag and Ag/SiO_2 NP samples after annealing (a,c) and XPS spectra of the Ag (b) and Ag/SiO_2 NP samples (d) before and after annealing.

presence of the SiO_2 shell additionally increases this distance which results in some loss of efficiency. **Figure 6** demonstrates that with decreasing the thickness of the SiO_2 shell (shown in the TEM image at each data point) the amount of PL enhancement measurably increases. The PL intensity for the NPs with 5 nm thick SiO_2 shell was found to increase by 2.2 times while for 2 nm thick SiO_2 NPs the enhancement was 2.8 times. Note that the density of Ag/SiO_2 NPs used in Figure 6 was approximately

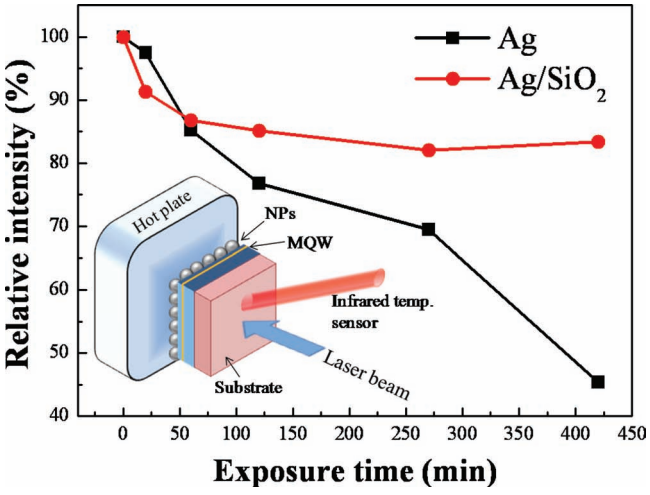

Figure 5. Peak PL intensity dependence on annealing time at 100 °C for the samples with Ag and Ag/SiO_2 NP coatings. The inset shows the schematic drawing of PL measurement system.

in the range of 2–3 × 10^{10} cm^{-2} and from Figure 3a this difference in concentration would not significantly influence the PL intensity. Because the energy transfer between the active layer and Ag/SiO_2 NPs is determined by the local enhancement of electromagnetic field near the active layer due to the LSP resonance, the thinning of the SiO_2 shell plays an important role in improving the quantum efficiency of LED.

This line of arguing, however, meets with certain problems when comparing the enhancement ratios for the samples coated with Ag NPs and Ag/SiO_2 NPs. Even though the distance of Ag NPs from the QW region is lower than for Ag/SiO_2 NPs, the amount of enhancement is approximately the same in both cases for high coverage density and for lower density the performance of the Ag/SiO_2 samples even exceeds that of their Ag NP counterparts (see Figure 3a,b). Also, according to general theory, the amount of PL increase due to LSP coupling should be equal to the ratio of fast relaxation lifetime components for uncoated and coated samples. This is indeed the case for the Ag/SiO_2 NP coated sample, but not for the Ag NP coated sample where the said ratio is considerably higher than the PL enhancement ratio. We believe that the reason is at least in part due to quantum tunneling between individual Ag NPs and nonlocal effects in dielectric screening for very low NP distances from the GaN spacer,[34,35] the effect that is strongly suppressed by the SiO_2 shell for Ag/SiO_2 NPs. In our version of sol-gel method the Ag NPs are covered by thin (2–3 nm thick) cetyl trimethyl ammonium bromide (CTAB),[36] but this thickness is apparently not enough for efficient suppression of tunneling. This CTAB coating is also apparently less efficient than the SiO_2 shell in preventing the NP coagulation during annealing.

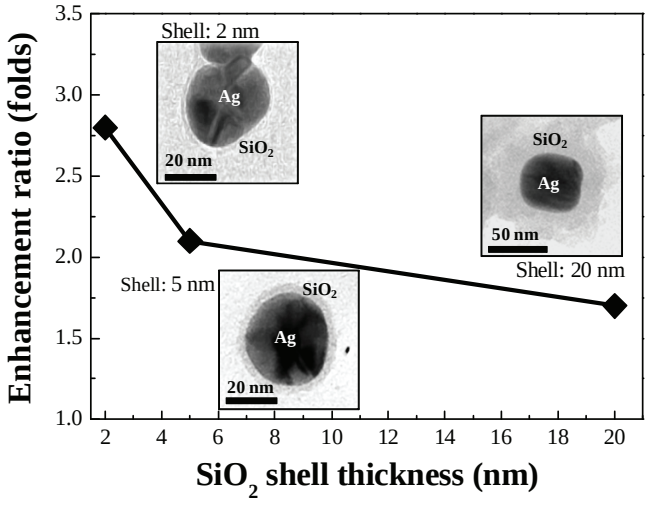

Figure 6. Dependence of experimental PL enhancement ratio on SiO_2 thickness in Ag/SiO_2 NPs coated on LED sample. The inset shows TEM images.

In addition, the amount of PL enhancement increases almost linearly with increasing the NP density in the case of Ag/SiO_2 NPs, as expected due to interaction between the electric fields of individual NPs.[19] In contrast, the dependence of PL enhancement ratio on NP density is markedly sublinear for Ag NPs.

3. Conclusions

Ag and Ag/SiO_2 NPs with chosen dimensions could be controllably and reproducibly prepared using a sol-gel method. Deposition of these NPs on top of GaN/InGaN MQW LED structures resulted in a strong increase of MQW PL efficiency, partly due to improved light extraction efficiency, but mostly because of the increase in internal quantum efficiency caused by the coupling of optical transitions in the MQW region to the LSP resonance. This coupling produced an additional recombination path that effectively suppresses the contribution of the non-radiative recombination channel and increases the IQE value. Numerical simulations predicted that the resonant wavelength of LSP related to Ag/SiO_2 NPs is located close to the wavelength of the blue emission of GaN/InGaN MQW structures, that the region of enhanced electric field due to LSP extends beyond the MQW region for structures with thin (≈10 nm) GaN spacer and that the expected amount of enhancement increases linearly with increasing the NP density. Experimental studies performed for Ag/SiO_2 and Ag NPs showed that in both cases a measurable (≈1.7 times) enhancement of the MQW PL efficiency could be achieved, but that for the Ag/SiO_2 NP coating the effect would be much more stable under the typical LED operation conditions (air ambient, active region temperature of ≈100 °C). The difference in behavior of the two types of NPs in that respect is due to an easier agglomeration and oxidation of the Ag NPs. For the Ag/SiO_2 NP coated sample the amount of PL enhancement increases with decreasing the thickness of the SiO_2 shell due to a decreased distance between the MQW and the Ag cores. The amount of PL enhancement changes linearly with density for Ag/SiO_2 NPs and sublinearly for Ag NPs. All in all, it is concluded that Ag/SiO_2 NPs provide a more predictable and stable PL performance than Ag NPs.

4. Experimental Section

InGaN/GaN LED Structure: The InGaN/GaN MQW structure was epitaxially grown by a metal organic chemical vapor deposition (MOCVD) technique. Trimethylgallium (TMGa), trimethylindium (TMIn), and NH_3 were used as precursors for Ga, In, and N, respectively. A thermal annealing of c-plane sapphire substrate was carried out at 1100 °C for 10 min, followed by the growth of a low temperature GaN buffer layer. A 400 nm-thick undoped GaN layer was grown at 1060 °C. Then, five InGaN/GaN MQW region was grown on high quality GaN epitaxial layer. The GaN barriers and InGaN wells were grown at temperatures of 850 °C and 750 °C, respectively. Finally, a 10 nm-thick undoped GaN layer was grown on top as a spacer layer.

Ag/SiO_2 Nanoparticles: The Ag/SiO_2 core/shell NPs were synthesized using a sol-gel method. A typical preparation procedure is as follows.[37] First, a 500 mL beaker was filled with 180 mL of aqueous solution including CTAB (0.145 g) under vigorous magnetic stirring. Next, a prepared aqueous solution of silver nitrate (0.1 M, 10 mL) was added to the mixed solution. And then, 20 mL of ascorbic acid (0.1 M) in aqueous solution was added to the mixture solution slowly within 5 min. After the mixture was further stirred for 10 min, sodium hydroxide (0.1 M) was added to accelerate the chemical reaction and the pH of the mixed solution was set at about 5. Subsequently, 50 mL of ethanol and, for the case of Ag/SiO_2 NPs, 1, 0.5 or 0.2 mL of tetraethoxysilane (TEOS), which controls the SiO_2 thickness, was added into the above-mentioned silver colloids. The solution was stirred for three more hours at room temperature (RT). In the case of Ag NP, the concentration of solution A was 1.5×10^{12} mL^{-1}, and solution B and C corresponded to the NP concentration of 1.9×10^{13} mL^{-1} and 1.6×10^{14} mL^{-1}, respectively. In the case of Ag/SiO_2 NPs, the concentration of solution D was 5.5×10^{11} mL^{-1}, and for solution E and F the concentration was 7.6×10^{12} mL^{-1} and 5.6×10^{13} mL^{-1}, respectively. The resulting mixture was drop-casted on the surface of the MQW structure and then dried for several seconds to form a layer of Ag or Ag/SiO_2 NPs.

FDTD Simulation: The full 3D FDTD simulation was performed to understand the electric field distribution of Ag/SiO_2 NPs. In the spatially digitized numerical simulation, minimum spatial size (grid size) should be small enough to resolve the field distribution, and 1-nm resolution in space (1 nm^3 in volume) was maintained. The diameter of Ag NPs was taken as 30 nm and the thickness of the SiO_2 coating (n = 1.55) was 20 nm. The 7 Ag/SiO_2 core/shell NPs were placed on top of GaN (n = 2.3). The perpendicularly polarized broad dipole source (center wavelength λ_c = 470 nm, bandwidth $\Delta\lambda$ = 60 nm) was positioned 10 nm below the contact point of GaN and Ag/SiO_2 NPs, which corresponds to the location of InGaN/GaN MQW in the structures.

Characterizations: The morphology of the Ag and Ag/SiO_2 NPs was investigated by high-resolution TEM (HR-TEM; JEOL, JEM 2100F) and SEM (JEOL, S4500). For room temperature and low-temperature PL measurements, the 325 nm line of a He–Cd laser with a 100 μm diameter and a 25 mW power was used as the excitation source. The PL measurement was performed through the back-side of sample, as shown in the inset of Figure 5. The NP coated samples were placed on the hot-plate with a gap of ≈50 μm and annealed at 100 °C. The sample temperature was monitored by infrared temperature sensor. TRPL was performed under pulse excitation of the InGaN/GaN based LED (pulse width of ≈5 ps, center wavelength of ≈405 nm) and the signals were analyzed by a monochromater, a photomultiplier tube, a high speed photodetector, and controller electronics. All decay lifetimes were calculated by the supplied software of Fluorescence Division.

Acknowledgements

This work was supported by the National Research Foundation of Korea (NRF) funded by the Korea government (MEST) (2010-0019626, 2010-0026614). J.-K. Y. acknowledges the support of Basic Science Research Program through the NRF funded by the Korea government (MEST) (2011-0015030).

Received: December 28, 2011
Revised: February 15, 2012
Published online: March 29, 2012

[1] W. L. Barnes, A. Dereux, T. W. Ebbesen, *Nature* **2003**, *424*, 824.
[2] K. A. Willtes, R. P. V. Duyne, *Annu. Rev. Phys. Chem.* **2007**, *58*, 267.
[3] A. V. Akimov, A. Mukherjee, C. L. Yu, D. E. Chang, A. S. Zibrov, P. R. Hemmer, H. Park, M. D. Lukin, *Nature* **2007**, *450*, 15.
[4] I. K. Ding, J. Zhu, W. Cai, S. J. Moon, N. Cai, P. Wang, S. M. Zakeeruddin, M. Gratzel, M. L. Brongersma, Y. Cui, M. D. McGehee, *Adv. Energy Mater.* **2011**, *1*, 52.
[5] P. Nagpal, N. C. Lindquist, S. H. Oh, D. J. Norris, *Science* **2009**, *325*, 594.
[6] K. Okamoto, I. Niki, A. Shvartser, Y. Narukawa, T. Mukai, A. Scherer, *Nat. Mater.* **2004**, *3*, 601.
[7] C. F. Lu, C. H Liao, C. Y. Chen, C. Hsieh, Y. W. Kiang, C. C. Yang, *Appl. Phys. Lett.* **2010**, *96*, 261104.
[8] M. Lunz, V. A. Gerard, Y. K. Gunko, V. Lesnyak, N. Gaponik, A. S. Susha, A. L. Rogach, A. L. Bradley, *Nano Lett.* **2011**, *11*, 3341.
[9] F. Tam, G. P. Goodrich, B. R. Johnson, N. J. Halas, *Nano Lett.* **2007**, *7(2)*, 496.
[10] D. M. Yeh, C. Y. Chen, Y. C. Lu, C. F. Huang, C. C. Yang, *Nanotechnology* **2007**, *18*, 265402.
[11] C. Y. Cho, S. J. Lee, J. H. Song, S. H. Hong, S. M. Lee, Y. H. Cho, S. J. Park, *Appl. Phys. Lett.* **2011**, *98*, 051106.
[12] M. K. Kwon, J. Y. Kim, B. H. Kim, I. K. Park, C. Y. Cho, C. C. Byeon, S. J. Park, *Adv. Mater.* **2008**, *20*, 1253.
[13] D. M. Yeh, C. F. huang, C. Y. Chen, Y. C. Lu, C. C. Yang, *Appl. Phys. Lett.* **2007**, *91*, 171103.
[14] C. Y. Cho, K. S. Kim, S. J. Lee, M. K. Kwon, H. D. Ko, S. T. Kim, G. Y. Jung, S. J. Park, *Appl. Phys. Lett.* **2011**, *99*, 041107.
[15] L. W. Jang, D. W. Jeon, T. Sahoo, D. S. Jo, J. W. Ju, S. J. Lee, J. H. Baek, J. K. Yang, J. H. Song, A. Y. Polyakov, I. H. Lee, *Opt. Express* **2012**, *20*, 2116.
[16] T. S. Oh, H. Jeong, Y. S. Lee, J. D. Kim, T. H. Seo, H. Kim, A. H. Park, K. J. Lee, E. K. Suh, *Appl. Phys. Lett.* **2009**, *95*, 111112.
[17] X. Gu, T. Qiu, W. Zhang, P. K. Chu, *Nanoscale Res. Lett.* **2011**, *6*, 199.
[18] R. F. Oulton, V. J. Sorger, T. Zentgraf, R. M. Ma, C. Gladden, L. Dai, G. Bartal, X. Zhang, *Nature* **2009**, *461*, 1.
[19] W. Sigle, J. Nelayah, C. T. Koch, P. A. van Aken, *Opt. Lett.* **2009**, *34*, 14.
[20] J. K. Yang, I. K. Hwang, M. K. Seo, S. H. Kim, Y. H. Lee, *Opt. Express* **2008**, *16*, 1951.
[21] P. B. Johnson, R. W. Christy, *Phys. Rev. B* **1972**, *6*, 4370.
[22] S. Linic, P. Christopher, D. B. Ingram, *Nat. Mater.* **2011**, *10*, 911.
[23] H. W. Huang, F. I. Lai, J. K. Huang, C. H. Lin, K. Y. Lee, C. F. Lin, C. C. Yu, H. C. Kuo, *Semicond. Sci. Technol.* **2010**, *25*, 065007.
[24] M. K. Lee, C. L. Ho, C. H. Fan, *Appl. Phys. Lett.* **2008**, *92*, 061103.
[25] K. Okamoto, I. Niki, A. Scherer, Y. Narukawa, T. Mukai, Y. Kawakami, *Appl. Phys. Lett.* **2005**, *87*, 071102.
[26] A. H. Chin, T. S. Ahn, H. Li, S. Vaddiraju, C. J. Bardeen, C. Z. Ning, M. K. Sunkara, *Nano Lett.* **2007**, *7*, 626.
[27] J. V. Foreman, J. Li, H. Peng, S. J. Choi, H. O. Everitt, J. Liu, *Nano Lett.* **2006**, *6*, 1126.
[28] M. H. Kim, M. F. Schubert, Q. Dai, J. K. Kim, E. F. Schubert, J. Piprek, Y. Park, *Appl. Phys. Lett.* **2007**, *91*, 183507.
[29] P. Benzo, L. Cattaneo, C. Farcau, A. Andreozzi, M. Perego, G. Benassayag, B. Pecassou, R. Carles, C. Bonafos, *J. Appl. Phys.* **2011**, *109*, 103524.
[30] Y. Han, R. Lupitskyy, T. M. Chou, C. M. Stafford, H. Du, S. Sukhishvili, *Anal. Chem.* **2011**, *83*, 5873.
[31] XPS International LLC, website: http://www.xpsdata.com (accessed November, 2011).
[32] A. D. McFarland, R. P. V. Duyne, *Nano Lett.* **2003**, *3*, 1057.
[33] K. L. Kelly, E. Coronado, L. L. Zhao, G. C. Schatz, *J. Phys. Chem. B* **2003**, *107*, 668.
[34] P. Anger, P. Bharadwaj, L. Novotny, *Phys. Rev. Lett.* **2006**, *96*, 113003.
[35] M. Thomas, J. J. Greffet, R. Carminati, J. R. Arias-Gonzalez, *Appl. Phys. Lett.* **2004**, *85*, 17.
[36] Z. M. Sui, X. Chen, L. Y. Wang, L. M. Xu, W. C. Zhuang, Y. C. Chai, C. J. Yang, *Physica E* **2006**, *33*, 308.
[37] K. Xu, J. X. Wang, X. L. Kang, J. F. Chen, *Mater. Lett.* **2009**, *63*, 31.